



The Stability Conditions of the Pump Structure Vibration

Nassir Hassan Abdul Hussain Al Hariri

Department of Machines and Equipment/Instate of Technology-Baghdad

(Received 27 March 2011; accepted 30 January 2012)

Abstract

The general approach of this research is to assume that the small nonlinearity can be separated from the linear part of the equation of motion. The effect of the dynamic fluid force on the pump structure system is considered vibrates at its natural frequency but the amplitude is determined by the initial conditions. If the motion of the system tends to increase the energy of the pump structure system, the vibration amplitude will increase and the pump structure system is considered to be unstable. A suitable MATLAB program was used to predict the stability conditions of the pump structure vibration. The present research focuses on fluid pump problems, namely, the role played by damping coefficient C , damping factor D and angular speed ω (termed the ratio $(\frac{\omega}{\omega_n})$) and the determining stability of a centrifugal pump structure. The data demonstrate substantial rotor dynamic effects, a destabilizing chart appears to be inversely proportional to the D , C , and ω , and resonance changes significantly with flow rate.

Keyword: Stability, Amplitude, Vibration, Resonance, Pump.

1. Introduction

Because of the complex spectra behavior of pump structure system it is not easy to interpret the results of pressure or velocity measurements of such systems [1]. The pump vibration comes from several sources that include mechanical causes of vibration, i.e. unbalanced rotating components, damaged impellers and non concentric shaft sleeves are common, non-laminar flow and operating the pump at a critical speed [2]. Frequencies below running speed can be caused by acoustical resonance. Generally these effects are due to the impeller passing and discharge diffuser [3]. Able to originate internally or externally, an excitation force is the only cause of vibration. Repeating forces create the vibration problems most commonly associated with centrifugal pump. These forces are often caused by the rotation of imbalanced, misaligned, or worn pump components [4]. However, in real structures the energy input by the flow has a finite limit, because the fluid forces on the structure are limited. Thus the amplitude of unstable region can

only grow until it is limited by nonlinearities in the structure itself [5]. Resonance can be avoided by changing a systems' frequency, which is determined by the mass, stiffness and damping properties of all of the components involved, including the pump, base, motor, piping-coupling, guard, foundation, etc. If the resonance vibration is just below the natural frequency, the stiffness of the system should be increased so the vibration frequency shifts above the natural frequency. If the resonance vibration is just above the natural frequency, the systems' mass should be increased, shifting the vibration frequency below the natural frequency [6]. Many vibration problems are results of interactions among a system pump, motor, fluid, piping and structure. This requires systems approach to vibration analysis, rather than the investigation of individual components [7]. A nonlinear system could have more than one equilibrium, some of which may be stable and others unstable as it is clearly noticed in the stability charts of the pump structure vibration[8].

2. Theory

The investigated equation of motion of the model pump structure in y-axis [9] is:

$$m\ddot{y} + (C - 3K_v)\dot{y} + Ky = F_f \quad \dots(1)$$

Let $a = \frac{C}{m} = \frac{2m\omega D}{m}$ and $b = K/m$

$$\ddot{y} + a\dot{y} + by - \frac{F_f}{m} = 0 \quad \dots(2)$$

To solve Eq. (2), a particular solution is assumed as:

$$y = Y \sin(\omega t)$$

Substituting Eq. (2) as:

$$-\omega^2 Y \sin(\omega t) + a \omega Y \cos(\omega t) + b Y \sin(\omega t) - \frac{F_f}{m} = 0 \quad \dots(3)$$

The stable and unstable regions of equation (3) depends on the parameters **a** and **b** and are shown in the charts of stability condition of the pump structure system.

Substituting and rearranging Eq. (3), the parameter **b** becomes:

$$b = \frac{F_f}{Y.m.\sin(\omega t)} + \omega^2 - a \omega \cot(\omega t) \quad \dots(4)$$

Substituting the values and after modifying and neglecting the small values of Eq.(1) the amplitude of the oscillating motion of the pump is obtained [9]:

$$Y = \frac{F_f}{K \sqrt{[1 - (\frac{\omega}{\omega_n})^2]^2 + [2D(\frac{\omega}{\omega_n})^2]^2}} \quad \dots(5)$$

By substituting values Y and K= m. ω^2 and substituting Eq. (5) in Eq. (4) as:

$$b = \frac{\sqrt{[1 - (\frac{\omega}{\omega_n})^2]^2 + [2D(\frac{\omega}{\omega_n})^2]^2}}{\sin(\omega t)} + 1 - \frac{a}{\omega} \cot(\omega t) \quad \dots(6)$$

The conditions of stability of the pump structure are given by the roots **a** and **b** as:

- b** > 0 stability is increased
- b** < 0 instability is increased
- a** > 0 always and pump structure system is stable

Equation (6) is known as the Mathieus equation [10].

The stable and unstable regions of Eq.(6) depends on the parameters **a** and **b** and are shown in the stability charts obtained. There are no known closed form solutions to the nonlinear differential equations describing the response of the pump structure used in an oscillating flow. It is possible to numerically integrate these nonlinear equations to obtain a solution.

At resonance $\omega = \omega_n$

If the frequency of the oscillating flow is much greater than the natural angular frequency of the structure, then the pump structure; becomes intensive to high frequency forces that energy in to the pump structure and cannot be transfer the response approaches zero [11].

Therefore the parameter **b** in Eq.(6) becomes:

$$b = \frac{\sqrt{2.D}}{\sin \omega_n} + 1 - \frac{a}{m.\omega_n} \cot(\omega_n t) \quad \dots(7)$$

The parameter **b** will be positive or negative depending actually upon the time of oscillating **t** and on the damping factor **D**.

The MATLAB program is used to solve the equation of motion (6) to get the stability charts. And reach the following assumptions:

$$r = (\frac{\omega}{\omega_n})^2$$

$$M = [1 - (\frac{\omega}{\omega_n})^2]^2$$

$$M = [1 - r]^2$$

$$S = [2.D. (\frac{\omega}{\omega_n})^2]^2$$

$$S = [2.D.r]^2$$

$$N = \sqrt{[1 - (\frac{\omega}{\omega_n})^2]^2 + [2D(\frac{\omega}{\omega_n})^2]^2}$$

$$N = \sqrt{M + S}$$

Substituting these values in Eq.(6) as:

$$b = \frac{N}{\sin(\omega t)} + 1 - (\frac{a}{\omega}) \cot(\omega t)$$

MATLAB Program

```
>> % We will now get Stability Condition at  $\omega=$ 
112
>> t=
0.001;0.002;0.003;0.004;0.005;0.006;0.007;0.008;
0.009;0.012;0.016;0.020;
>> r =
0.221;0.307;0.469;0.623;0.854;1;112;1.44;1.74;1.
94;2.175; 2.509;
>> D =
0.01;0.06;0.10;0.15;0.25;0.35;0.40;0.55;0.65;0.75
;0.85;0.95;
>> a = 2 *  $\omega$  * D;
>> a
>> M = (1-r)^2
>> M
>> S = (2*D*r)^2
>> S
>> N = sqrt (M+S)
>> N
>> b= N/sin( $\omega$  *t)+1-(a/  $\omega$ )*cot( $\omega$  *t)
>> b
```

To draw the stability charts of the pump structure at different values of times, ratios of angular speeds with natural speed and damping factors, the MATLAB program was used:

```
>> % We will give variables for plot at  $\omega=$  112
>> a=[ 2.24; 13.4; 22; 33; 56; 78; 89; 123; 145;
168; 190; 212];
>> b=[ 7.79; 3.98; 2.79; 2.18; 1.68; 1.39; 1.32;
1.16; 1.161; 1.52; 2.26; 3.63];
>> % We will plot
>> plot (a,b,'-ob','LineWidth',2,'MarkerSize',1)
>> xlabel('a')
>> ylabel('b')
>> title('\bf Stability Condition')
```

The MATLAB program of the stability condition at resonance state where

$\omega = \omega_n = 238$ is:

```
r= 1
M= 0
>> % We will now get Stability Condition at
resonance state  $\omega = \omega_n = 238$ 
>> t =
0.001;0.002;0.003;0.004;0.005;0.006;0.007;0.008;
0.009;0.012;0.016;0.020;
>> D = 0.01; 0.06; 0.1; 0.15; 0.25; 0.35; 0.40;
0.55; 0.65; 0.75; 0.85; 0.95;
>> a= 2*  $\omega_n$  * D;
>> S= (2*D)^2;
>> S
>> N= 2*D;
```

```
>> b= N/sin(238 *t)+1-(a/ 238)*cot(238*t);
>> b
```

The MATLAB program to plot the stability condition at $\omega = 132$ is:

```
%% WE will now give the variable for plot1 of
stability chart at  $\Omega = 132$ 
a=[2.64;15;26;39;66;92;105;145;171;198;224;250
];
b=[6.11;3.21;2.32;1.87;1.51;1.32;1.31;1.26;1.33;1
.85;3.03;6.34];
%Now we will plot the plot1 of stability at
omega=132
plot(a,b,'-ob','LineWidth',2,'MarkerSize',2)
% WE will give values for plot2 of experimental
a=[2.64;15;26;39;66;92;105;145;171;198;224;250
];
b=[0;3;4.3;3.9;3.6;2.5;6.3;5.8;4.5;6.9;7.8;9.1];
% We will plot plot2 of experimental
% but we must use hold command to be able to
show the the plot2 at the same window
hold on
plot(a,b,'--*r','LineWidth',2,'MarkerSize',2)
% We will give values for plot3 at resonance
a=[4.76;28;47;71;119;166;190;261;309;357;404;4
52];
b=[1;1.02;1.07;1.15;1.33;1.60;1.88;2.54;3.38;11;-
3.9;-0.81];
%% We will plot for plot3 at resonance
plot(a,b,'-.+k','LineWidth',2,'MarkerSize',2)
xlabel('a')
ylabel('b')
legend('132','exp','res',0)
```

Displacement amplitudes are used at low vibration frequencies typically between (17-62) Hz. High displacement amplitudes at low frequencies can cause a considerable amount of stress damage to a pump structure. Using MATLAB program determined the stability conditions at angular speeds $\omega = [112, 132, 163, 188, 220, 238, 251, 286, 314, 332, 351, 377]$. And MATLAB program was used also to plot the stability conditions of the pump structure at these angular speeds.

Fig.2.indicates the particular stability condition at angular speed $\omega = 112$. It has two small regions of stability and large area of instability. It is nearly similar to stability in Fig.3. in which it is at angular speed $\omega = 132$ at the ratios of angular speeds (ω / ω_n)=(1/2.1 and 1/1.8).

3. Experimental method

The measurements method was tested on laboratory test instrument “Pumps Training System lab-volt”. The photographic picture of the research experiment is shown in Fig.1. In the laboratory test, water is circulated from the water tank. The speed is measured by using an electromagnetic flow meter. The static pressure is measured, relative to atmospheric pressure at the suction and discharge flanges of the pump. When operating the pump will act as an active element in the test loop . In this experiment pump induced pulsations are suppressed by coherence analysis with the external source signal as a reference. Measurements should be taken at operating speed for constant speed motor and at varying speeds for pump operating on variable speed drives [12].



Fig. 1. The Photographic Picture of the Research Experiment [9].

This research is carried out by using the type of centrifugal non-positive displacement, which has two kinds of openings; one opening is for flow- drag and the other opening is for flow-pushing. The drag opening is connected with fluid tank, and the pushing opening is joined with flow-meter to measure the fluid flow discharge. Then there is a valve for hindering the fluid flow which is coupled with its valve adjustment in parallel. The motor is linked with the pump, and the regulation is lying on the motor speeds by varying the frequencies. It takes the readings of the fluid flow discharge, and the pressure readings are

taken by the manometer. The readings of the vibration amplitudes of the pump structure are taken by the vibrometer, and the rpm of the propeller of the pump are also taking. The readings are shown in the Appendix of Table.1. and Table.2.

The value of the natural angular speed $\omega_n=238$ is determined by using the Analyzer.

Table1,
The Measured Parameters of the Fluid Flow in the Pump [9].

Frequency F [Hz]	Angular speed ω [rad/s]	Vibration Amplitude RMS	Speed of Pump [rpm]
0	0	0	0
17.9	112	3	1029
21	132	4.3	1207
26	163	3.9	1495
30	188	3.6	1725
35	220	2.5	2012
38	238	6.3	2185
40	251	5.8	2300
45	283	4.5	2587
50	314	6.9	2875
55	345	7.8	3162
60	377	9.1	3450

Table2,
Shows the Measured and Calculated Parameters of the Pump Structure [9].

Total mass m [kg]	Measured mass m_o [kg]	Entrained mass m_f [kg]	Cross-sec. of pump A [m ²]
7.2	1.2	6	0.00567
Stiffness of pump K [N.s/m]	Measured angular speed of pump ω_n [rad/s]	Width of pump B [m]	Diameter of pump d [m]
47203	238	0.0265	0.085

4. Results and Discussion

Figure (4) Shows the stability chart taking another form with small increasing in the zone of stability at angular speed ratio (1/1.26). Fig.5 the area of stability decreases to some values, then the curve increases sharply to some extent. In Fig.6. and Fig.7. show the stability charts reduce at angular speed ratios more than one, i.e. ($\omega/\omega_n = 1/0.94$ and $1/0.75$), they are very close to each others. It is concluded from the figures that the stability charts depend on the effect of the time of occurring of the vibration of the pump structure, in which parameter **b** plays the main role than the other parameters. It means that at the time occurring the amplitude of vibration at natural angular speed $\omega_n = 238$ was higher than that of the lower angular speeds. However, it was predicted that the time of vibration amplitudes at lower frequencies were near zero values, which gave almost straight line at zero line of **b** parameter. The parameter **b** is playing a more important role than the values of **a** parameter at all values of the angular speeds, because the values of **a** parameter are always positive, while the values of **b** parameter are positive or negative values; they depend on the values of the times of vibration amplitudes.

The stability charts are obtained in the figures, by keeping natural angular speed ω_n and some other parameters are constants and then varying angular speed ω to vary the ratio ω/ω_n . It will be noticed actually, if the horizontal shaft is run at angular speed lower than natural angular speed $\omega_n = 238$, then it will be instabilized at angular speeds 112, 132, and 163 which are nearly equal to half value of natural angular speed as shown in Figures 2, 3, and 4. In Figures 5, 6, and 8, the behavior of the stability charts are different at angular speeds 188, 220 and 251 because the stable areas were noticed evidently at negative **b** parameter, if the variable damping factor is assumed with constant value of the stiffness.

It is concluded also from the figures of stability charts, that the region between curves of theoretical stability charts at $\omega=(112$ and $132)$ and of resonance chart at $\omega_n = 238$ is called critical zone, which here it represented in small area. But at $\omega = (163, 188, 220, 251$ and $286)$ critical zone coincides at the same line of each curve for certain extent of values of parameter **a** which is always positive. However, this means the system of the pump structure has the same critical limit. Then with th increasing the values of $\omega = (314, 332, 351$ and $377)$ the possibility of the critical

zone begins to increase gradually for small area also at positive values of parameter **b**.

The ratio of error between the theoretical and experimental is between (0.2590 and 0.1403) for $\omega=(112 - 377)$.

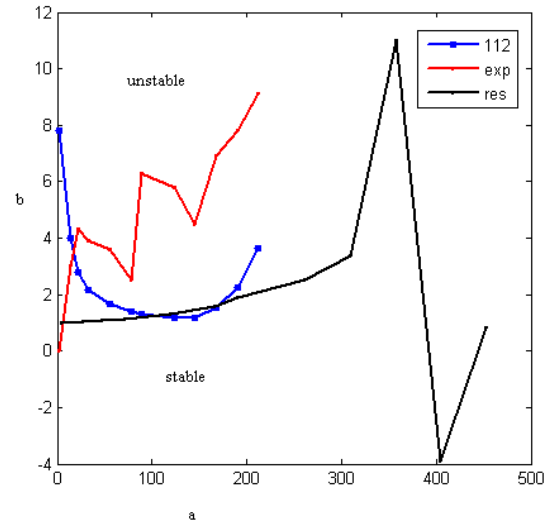


Fig. 2. Stability chart at $\omega= 112$.

When blue line represents $\omega= 112$,red line exp. represents experimental ,black line res. represents resonance.

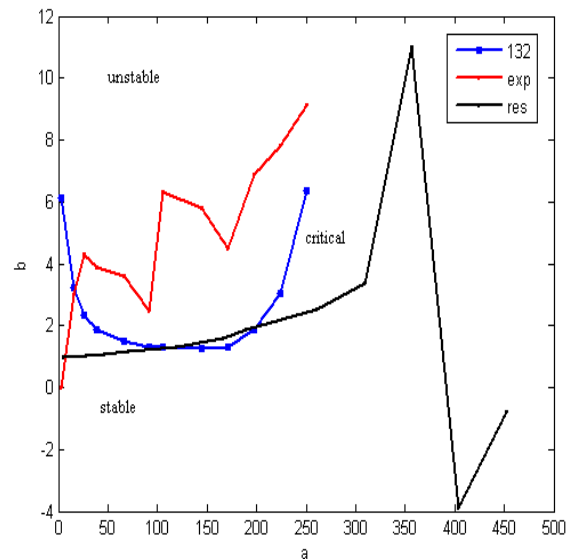


Fig. 3. Stability chart at $\omega= 132$.

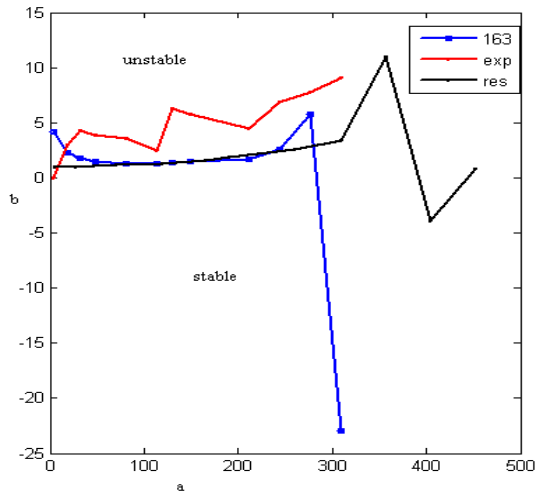


Fig. 4. Stability chart at $\omega=163$.

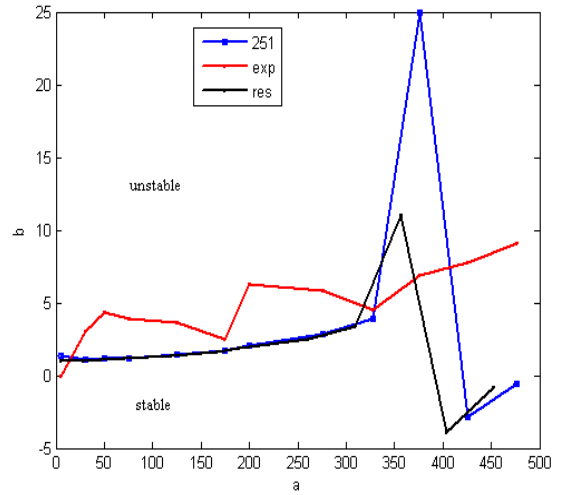


Fig. 7. Stability chart at $\omega=251$.

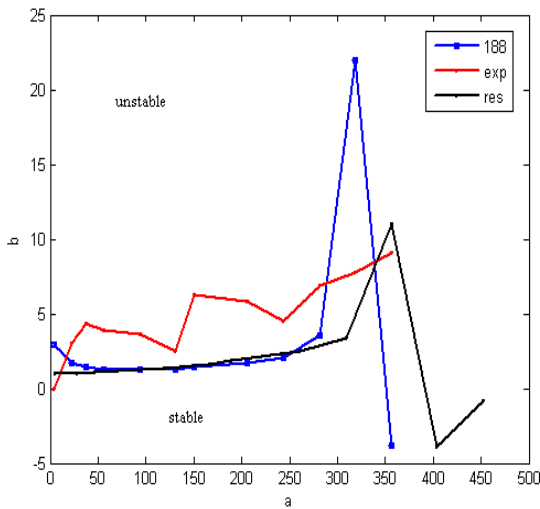


Fig. 5. Stability chart at $\omega=188$.

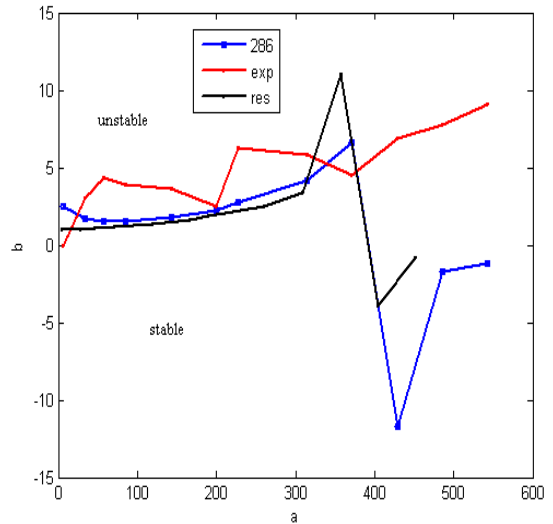


Fig. 8. Stability chart at $\omega=286$.

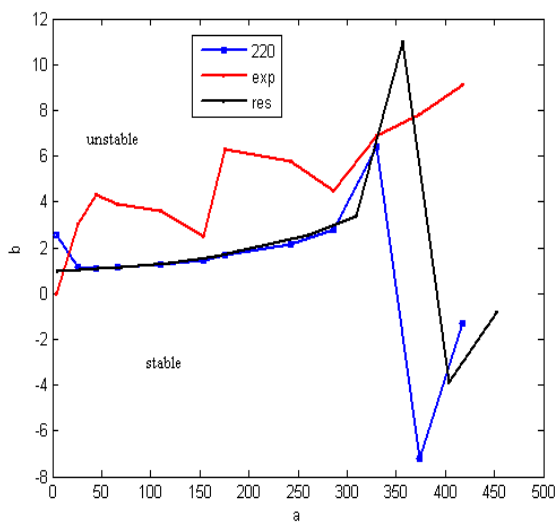


Fig. 6. Stability chart at $\omega=220$.

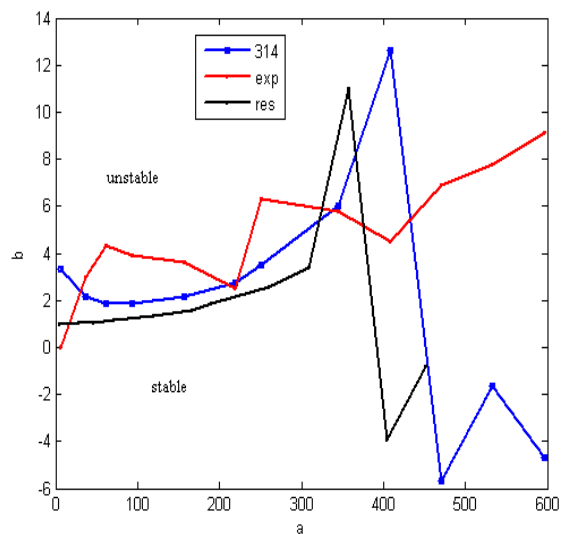


Fig. 9. Stability chart at $\omega=314$.

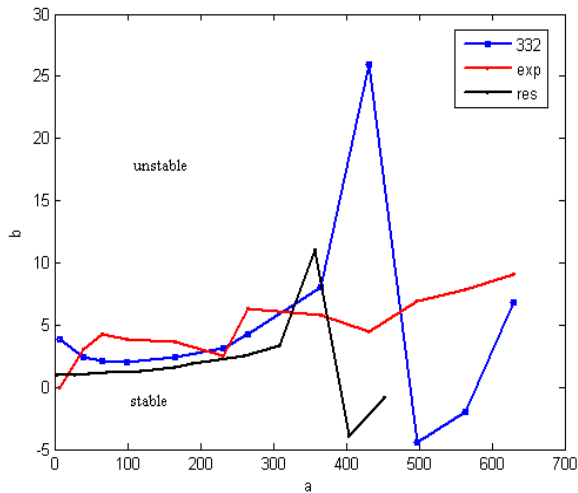


Fig. 10. Stability chart at $\omega= 332$.

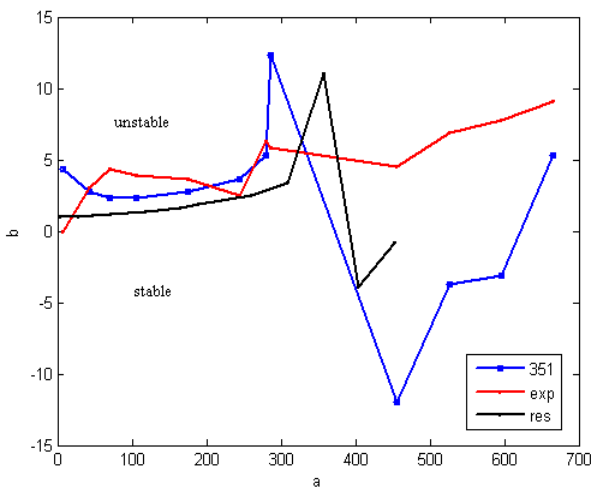


Fig.11. Stability chart at $\omega= 351$.

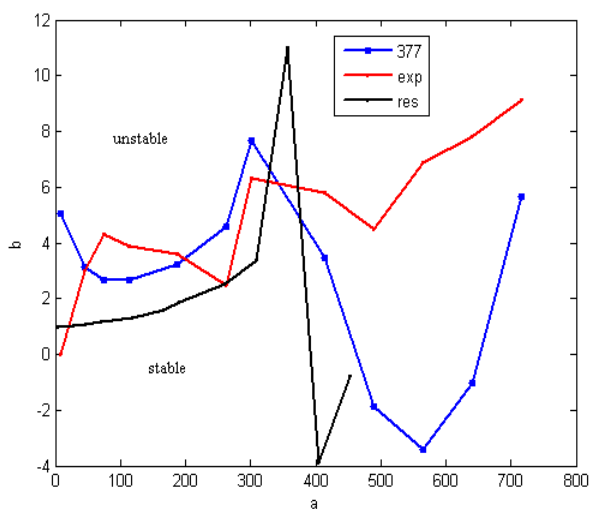


Fig. 12. Stability chart at $\omega= 377$.

5. Conclusions

From the results obtained the following conclusions can be withdrawn:

- 1- The stable and unstable regions of the equation of motion Eq.(6) depend on the parameters **a** and **b** which are shown in the stability charts figures.
- 2- Very small values for time of vibration amplitudes are required to get accepted results. If time **t** was not sufficiently small, the results would be very inaccurate.
- 3- The accuracy of the procedure increases as the value of the dynamic fluid force and damping forces decrease relative to the inertial and spring forces in the equation of motion.
- 4- Parameter **b** played a more important role than parameter **a** at values of angular speeds, naturally, because the parameter **b** depends on angular speeds, dynamic fluid force, damping factors and different values of time of vibration amplitudes.
- 5- It is noticed that the effect of pump structure damping is important near the ratio ω/ ω_n which is between 0.45 and 1.58.
- 6- It is pointed out that a typical swirl velocity ratio at inlet (pump discharge) would be about 0.65 and may not be therefore large enough for the resonance to be manifest.

Nomenclature

- m total mass of the model pump structure [kg]
- C damping coefficient of the pump structure [N.s/m]
- K_v fluid force velocity coefficient [N.s/m]
- K stiffness of the pump structure [N/m]
- F_f total fluid force [N]
- ω measured angular speed of the pump [rad/s]
- ω_n natural angular speed of the blades of the model pump structure immersed in the fluid [rad/s]
- f frequency of the pump structure [Hz]
- D damping factor of the pump

6. References

- [1] JONG CHRISTIAAN ARNOLDUS FRACISCUS DE, "Analysis of Pulsations and Vibrations in Fluid – Filled Pipe System", Eindhoven University of Technology, Thesis Eindhoven – ref. ISBN 90 – 386 – 0074 – 7, 1994.
- [2] www.mcnallyinstitute.com.
- [3] www.scribd.com.
- [4] HPAC ENGINEERING, " Applications & Resources Pumping and Piping, Examining Causes of Pump Vibration", April 2009.
- [5] FRANCES, TSE, IVAN MORSE & ROLLAND T. HINPLE, " Mechanical Vibrations Theory and Applications", Pub. ALLYN and Bacon, Sc. 1998.
- [6] BILL WATTS and JOE VAN DYKE, " An Automated Vibration-Based Expert Diagnostic System", Sound & Vibration, Sept. 1993.
- [7] <http://en-wikipedia.org/wiki/pump>.
- [8] BILL WATTS, " Triaxial Vibration Spectral Data, An Important Ingredient for Proper Diagnosis", DLI Engineering, 253 Winslow Way West, Bainbridge Island, WA, 1998.
- [9] NASSIR HASSAN ABDUL HUSSAIN, "The Effect of Fluid Force on The Pump Structure Vibrations", Second Scientific Conference of the College of Engineering-University of Al – Qadisiya, pp. 420-435, 19-20 Oct. 2009.
- [10] WILLIAM F. THOMSON, " Vibration Theory and Application, George Alien and Anwin LTD, London, 1995.
- [11] YOSHIDA, Y. , MURAKAMI, Y. , TSURUSAKI, T. AND TSUJIMOTO, Y. " Rotating Stalls in Centrifugal Impeller / Vaned Diffuser System", Proc. First ASME / JSME Joint Fluids Eng. Conf. , FED-107, 125-130, 1991.
- [12] PUMP TRAINING SYSTEM LAB-VOLT, No. 4606, Work Orders-Instruc. 37894-20, USA, 2004.

حالة الإتران لإهتزاز هياكل الضاغظ

ناصر حسن عبد الحسين الحريري

قسم المكاتن والمعدات/ معهد التكنولوجيا - بغداد

الخلاصة

لفهم الطريقة العامة للبحث فقد فرض قليل من الجزء الغير خطي بأن يفصل من الجزء الخطي لمعادلة الحركة. ولقد أخذت بنظر الإعتبار تأثيرات قوة السائل الديناميكية على نظام هيكل الضاغظ، حيث أنه يهتز عند الذبذبات الطبيعية ولكن بحسب المدى من الشروط الأولية. إذا كان نظام الحركة يميل لزيادة الطاقة لنظام هيكل الضاغظ، فسوف يزداد مدى الإهتزاز ويعتبر نظام هيكل الضاغظ غير متزن. لقد أستخدم نظام MATLAB المناسب لتخمين حالة الإتران لإهتزاز هيكل الضاغظ. البحث الحالي يركز على مشاكل السائل للضاغظ، إسمياً للدور الحادث بواسطة معامل التخميد C، عامل التخميد D، والسرعة الزاوية (التي عبرت بالنسبة $(\frac{\omega}{\omega_n})$) وكذلك في حساب الثباتية والصفة المميزة لهيكل الضاغظ ذو الطرد المركزي. البيانات تظهر بوضوح التأثيرات الحقيقية للمحور الدوار الديناميكي، ومنحنيات عدم الإتران تظهر العلاقة العكسية مع ω , C, D، وكذلك الرنين يتغير بشكل كبير مع معدل الجريان.